

See discussions, stats, and author profiles for this publication at: <https://www.researchgate.net/publication/280579604>

# Properties enhancement using oil palm shell nanoparticles of fibers reinforced polyester hybrid composites

Article in *Advanced Composite Materials* · July 2015

CITATIONS

0

READS

187

4 authors:



**Enih Rosamah**

Universitas Mulawarman

16 PUBLICATIONS 48 CITATIONS

[SEE PROFILE](#)



**Md Sohrab Hossain**

University of Kuala Lumpur

57 PUBLICATIONS 330 CITATIONS

[SEE PROFILE](#)



**Abdul Khalil H.P.S**

Universiti Sains Malaysia

219 PUBLICATIONS 5,258 CITATIONS

[SEE PROFILE](#)



**Rudi Dungani**

Bandung Institute of Technology

55 PUBLICATIONS 634 CITATIONS

[SEE PROFILE](#)

Some of the authors of this publication are also working on these related projects:



biocomposite from waste biomass [View project](#)



Nanocellulose from lignocellulose biomass [View project](#)



## Properties enhancement using oil palm shell nanoparticles of fibers reinforced polyester hybrid composites

Enih Rosamah, Md. Sohrab Hossain, H.P.S. Abdul Khalil, W.O. Wan Nadirah, Rudi Dungani, A.S. Nur Amiranajwa, N.L.M. Suraya, H.M. Fizree & A.K. Mohd Omar

**To cite this article:** Enih Rosamah, Md. Sohrab Hossain, H.P.S. Abdul Khalil, W.O. Wan Nadirah, Rudi Dungani, A.S. Nur Amiranajwa, N.L.M. Suraya, H.M. Fizree & A.K. Mohd Omar (2016): Properties enhancement using oil palm shell nanoparticles of fibers reinforced polyester hybrid composites, *Advanced Composite Materials*, DOI: [10.1080/09243046.2016.1145875](https://doi.org/10.1080/09243046.2016.1145875)

**To link to this article:** <http://dx.doi.org/10.1080/09243046.2016.1145875>



Published online: 01 Mar 2016.



Submit your article to this journal [↗](#)



Article views: 34



View related articles [↗](#)



View Crossmark data [↗](#)

## Properties enhancement using oil palm shell nanoparticles of fibers reinforced polyester hybrid composites

Enih Rosamah<sup>a</sup>, Md. Sohrab Hossain<sup>b</sup>, H.P.S. Abdul Khalil<sup>b,c,\*</sup>, W.O. Wan Nadirah<sup>b</sup>, Rudi Dungani<sup>d</sup>, A.S. Nur Amiranajwa<sup>b</sup>, N.L.M. Suraya<sup>b</sup>, H.M. Fizree<sup>b</sup> and A.K. Mohd Omar<sup>b</sup>

<sup>a</sup>Faculty of Forestry, Mulawarman University, Campus Gunung Kelua, Samarinda 75119, East Kalimantan, Indonesia; <sup>b</sup>School of Industrial Technology, Universiti Sains Malaysia, 11800 Penang, Malaysia; <sup>c</sup>Institute of Tropical Forestry and Forest Products (INTROP), Universiti Putra Malaysia, 43400 Serdang, Selangor Darul Ehsan, Malaysia; <sup>d</sup>School of Life Sciences and Technology, Institut Teknologi Bandung, Gedung Labtex XI, Jalan Ganesha 10, Bandung 40132, West Java, Indonesia

(Received 26 March 2015; accepted 13 July 2015)

Oil palm shell (OPS) nanoparticles were utilized as filler in fibers reinforced polyester hybrid composites. The OPS nanoparticles were successfully produced from the raw OPS using high-energy ball milling process. Fundamental properties including morphology, crystalline size, and particle size of the OPS nanoparticles were determined. Tri-layer natural fiber reinforcement (kenaf-coconut-kenaf fiber mat) polyester hybrid composites were prepared by hand lay-up techniques. The influences of the OPS nanoparticles loading in the natural fibers reinforced polyester hybrid composites were determined by analyzing physical, mechanical, morphological, and thermal properties of the composites. Results showed that the incorporation of the OPS nanoparticles into the hybrid composites enhanced the composite properties. Further, the natural fibers reinforced polyester hybrid composite had the highest physical, mechanical, morphological, and thermal characteristics at 3 wt.% OPS nanoparticles loading.

**Keywords:** Hybrid composite; Natural fiber; Polymer-matrix composites; Mechanical properties; Physical properties

### 1. Introduction

With increasing ecological safety concern, the natural fibers are increasingly in demand across a wide range of polymer composite application.[1] Natural fiber offers potential advantages over synthetic fibers such as abundant availability, low cost, low density, degradable, and renewability, which turns the natural fiber as a potential replacement of synthetic fibers to be used as a filler/reinforcement in polymer composites.[1–3] Studies reported that the utilization of natural fiber as reinforcement materials in polymer composites would minimize materials cost and make the composite partially biodegradable.[2–8] Taking into consideration raising environmental awareness, natural fibers can be considered as the most promising material in advanced composites engineering applications.[9]

---

\*Corresponding author. Email: [akhalil@usm.my](mailto:akhalil@usm.my)

In a hybrid composite, two or more reinforcements are utilized into a single matrix to gain the composite properties diversity.[10] Therefore, designing the hybrid composite with apposite combination of reinforcements and filler is urged to gain superior strength performance in numerous innovative applications.[11] The performances of hybrid composites primarily rely upon the fiber content, length of individual fibers, orientation, extent of intermingling of fibers, fiber to matrix bonding, and homogenous distribution of fibers reinforcement and filler matrix into the composite.[7,11] Studies have been conducted on the preparation and characterization of hybrid composites using thermoplastic matrix as reinforcement and conventional fillers.[12–14] Wherein, nanoparticles are being utilized as an alternative tool for enhancing mechanical and thermal properties of natural fiber-reinforced polymer composites.[15–17] Therefore, a few studies have been conducted using nanostructured particles as filler.

Nanoparticles, due to nanosize, would offer the matrix high surface area. However, the utilization of inorganic nanoparticles in polymer composite is challenging, since the homogenous dispersion of inorganic nanoparticles into the polymer matrix is difficult to ensure.[15,18] Inorganic nanoparticles have a tendency to agglomerate. Therefore, the use of inorganic nanoparticles as a filler might lead the materials to deterioration thereby, decreasing the mechanical and thermal properties of polymer composite.[7,19] Besides, synthetic fibers arise ecological concern and health hazard to the personnel involved in the manufacturing composites.[20,21] In recent years, lignocellulosic materials have been utilized as an alternative for conventional fiber in the development of polymer composite due to their environmentally friendly nature. However, the use of lignocellulosic materials in fiber-reinforced polymer composite has certain limitations, including poor fiber/matrix interactions, water resistance, and relatively lower durability.[22,23] The weak interfacial bonds between highly hydrophilic natural fibers and hydrophobic non-polar organophilic polymer matrix might lead to a considerable decrease in physical, thermal, and mechanical properties of composite. There are several approaches that could be applied to overcome the deficiency of the natural fiber matrix compatibility including the introduction of nanoparticles into the fiber matrix.[15,24]

The oil palm shell (OPS) is a lignocellulosic material, which is considered as agricultural waste.[25] Usually, OPS is burned or used as cover on the surface of the roads in the plantation area. Although, the incorporation of nanoparticles in fiber-reinforced polymer matrix has the possibility to gain optimal composite performance,[26] combination of filler–resin with three-phase fiber-reinforced composites is still in infancy. Therefore, the present study was conducted to produce three-phased hybrid polyester composite. Wherein, the OPS nanoparticles were utilized as filler in order to enhance the mechanical, physical, thermal, and morphological properties of the prepared natural fiber-reinforced hybrid composite.

## 2. Materials and methods

### 2.1. Materials

Woven kenaf fiber mat ( $250 \times 200 \text{ mm}^2$ ) used in this research was procured from Nibong Tebal Paper Mills, Seberang Prai, Penang, Malaysia. Coconut fiber mat ( $250 \times 200 \text{ mm}^2$ ) used in this research was provided by Ecofiber Technology Sdn. Bhd, Malaysia. The OPS chips were collected from Ulu Keratong palm oil mill, Segamat,

Johor, Malaysia. Unsaturated polyester resin P9509 and methyl ethyl ketone peroxide (MEKP) were obtained from Euro Chemo-Pharma Sdn. Bhd, Malaysia.

## 2.2. Preparation of OPS nanofiller

The collected OPS chips were converted into granular particles by grinding in the Wiley mill. Subsequently, OPS granular was sieved (60 mesh size) to separate micro-sized particles such as sand, stones, and micro particle from the mill. Sieved OPS granular was then oven dried in an oven at 110 °C for 24 h to reduce its moisture content. The dried OPS granular was ground and further sieved to a particle size fraction range of 2–2.8 mm. Fine OPS powder (total evaporable moisture content of 1.50%) was further grounded using high-energy ball milling process at 170 rev min<sup>-1</sup> for 30 h. Wherein, the ball mill was filled with a ball-to-powder weight ratio of 10:1 in a stainless steel chamber using stainless steel balls (diameter: 19 mm × 12.7 mm × 9.5 mm). The samples were then oven dried at 110 °C for 24 h to prevent agglomeration and avoid contact with moisture.

## 2.3. Characterization of OPS nanoparticles

The morphology of OPS nanoparticles was determined using scanning electron microscope (SEM) (Model: EVO MA10, Carl ZEISS). The samples were placed onto SEM holder using double-sided electrically conducting carbon adhesives tapes to avoid surface charge on the specimens, when exposed to the electron beam. The specimen was then coated with a thin gold palladium layer using sputter coater Polaron SC515. The SEM micrographs were obtained under conventional secondary electron imaging conditions with an accelerating voltage of 5 kV. The energy dispersion of SEM analysis of the OPS nanoparticles was conducted by Leica Cambridge S-360 SEM.

A Fourier transform infrared spectroscopy test was carried out to examine functional groups present in OPS nanoparticles. About 1 mg of OPS nanoparticles was mixed with 100 mg of KBr powder. Then, the powder mixtures were pressed into transparent thin pellets. Spectral outputs were recorded in the transmittance as a function of wave number and represented in a graph.

X-ray diffraction (XRD) (D8 Advanced, Bruker, Germany) analysis was performed using Cu-K $\alpha$  radiation at 40 kV and 25 Ma and  $\lambda = 1.54 \text{ \AA}$ . About 2 g of OPS nanofiller was run at a scan ratio of 0.05 degree/s. The X-ray pattern was recorded in  $2\theta$  values range of 10°–90°. The crystallinity index (CI) was calculated using the following equation:

$$\text{CI (\%)} = \frac{I_{200} - I_{AM}}{I_{200}} \times 100 \quad (1)$$

where  $I_{200} - I_{AM}$  is the height ratio between the intensity of the crystalline peak, and  $I_{200}$  is the total intensity.

The particle size of OPS nanoparticles was measured using transmission electron microscope (TEM) image and particle size distribution analyses. The dried OPS nanofiller was dissolved in acetone and dispersed with an ultra sonicator for 10 min. Next, the sample was placed on copper grids and cloud with 2% uranyl acetate and Reynold's lead citrate. Finally, copper grids containing 0.1  $\mu\text{m}$  samples were viewed under TEM (energy filter – Zeiss Libra® 120) at certain magnifications. Particle size distribution of OPS nanoparticles was assessed on a MALVERN Zetasizer Ver. 6.11, serial number:

MAL 1029406 Nano Series by dynamic light scattering measurements by means of 532 nm laser. The analysis was repeated three times according to the equipment internal setting.

The thermal properties of OPS nanoparticles were assessed by means of simultaneous thermogravimetric and differential thermogravimetric analyses (TGA) using a Perkin Elmer thermal gravimetric analyzer Pyris 1 TGA. About 4–5 mg of OPS nanofiller was distributed evenly in an open platinum crucible used and heated from 30 to 800 °C under nitrogen at a heating rate of 10 °C/min.

#### 2.4. Preparation of polyester hybrid composites

OPS nanofiller/polyester matrix was prepared by adding OPS nanoparticles (1–5%) into the polyester resin and then mixed using a mechanical stirrer for 15 min at 200 rpm prior to adding 1% MEKP as a curing agent. Tri-layer hybrid composites (kenaf–coconut–kenaf) were prepared by keeping total fiber loading of both fibers at 40% by following hand lay-up techniques. Subsequently, the prepared hybrid composites were immersed into OPS nanofiller/polyester matrix until the fibers melted. A stainless steel mold with dimensions 250 mm × 200 mm × 7 mm was used for soaking the fiber mats. Then, the molds were closed for cold press at 200 psi, and subsequently cured at room temperature for 24 h. Pure hybrid composite without filler was also prepared as a control.

#### 2.5. Analysis of enhancement properties of fibers reinforced polyester hybrid composites

##### 2.5.1. Physical properties

Composite density was measured according to the ASTM standard.[27] Composite samples were cut into dimensions of 30 × 20 × 7 mm<sup>3</sup> according to the standard prior to calculating the density. The density of the samples was calculated following Equation (2). The results were expressed as average value of five experimental runs.

$$\text{Density (g cm}^{-3}\text{)} = \frac{m}{v} \quad (2)$$

where  $m$  is the mass of the composites (g),  $v$  is the volume of the composites (m<sup>3</sup>).

The void content in the prepared hybrid composites was determined according to ASTM standard 1999 [28] as follows:

$$\text{Void content (\%)} = \frac{\rho_{\text{theoretical}} - \rho_{\text{experimental}}}{\rho_{\text{theoretical}}} \quad (3)$$

wherein the *theoretical* density was calculated as:

$$\rho_{\text{theoretical}} = \frac{1}{\frac{W_f}{\rho_f} + \frac{W_m}{\rho_m}} \quad (4)$$

where  $W_f$  is the reinforcement weight fraction,  $W_m$  is the matrix weight fraction,  $\rho_f$  is the reinforcement density, and  $\rho_m$  is the matrix density.

### 2.5.2. Mechanical properties

Tensile test was performed using INSTRON 5582 universal testing machine. A rectangular composite sample with dimensions  $120 \times 20 \times 7 \text{ mm}^3$  was used as per ASTM 2000 standard.[29] The gage length was set at 60 mm with a crosshead speed of 5 mm/min. Tensile properties including tensile strength, modulus, toughness, and elongation at break were acquired from data recorded. In each case, five specimens were tested and the average value was tabulated.

Flexural properties including strength, modulus, and toughness were determined by following three-point flexural testing method in accordance with ASTM 2003 standard.[30] The test was carried out using INSTRON (Model 5582) universal testing machine. The crosshead speed was 2 mm/min. Izod notched impact testing was performed using GEOTECH testing machine (Model GT-7045 MD). The impact strength was determined according to ASTM 2006 standard method.[31]

### 2.5.3. Morphology properties

SEM was used to determine the tensile fracture surface of the hybrid biocomposite. The test sample was coated with a thin gold palladium layer using sputter coater polaron SC515 to prevent electrical charge accumulation during examination. The fiber–matrix adhesion was then studied using SEM. The SEM micrographs were obtained under conventional secondary electron imaging conditions with an accelerating voltage of 5 kV.

### 2.5.4. Thermal properties

A Perkin Elmer thermal gravimetric analyzer Pyris 1 was used to study the thermal stability of the composites. The powder of composites (about 5 mg) was distributed evenly in an open platinum crucible used and heated from 30 to 800 °C under a nitrogen atmosphere with a heating rate of 10 °C/min.

## 3. Results and discussion

### 3.1. Characterization of OPS nanoparticles

The SEM images revealed that OPS nanoparticle were crushed with irregular structural shape (Figure 1(a)). This happened probably due to the preparation of OPS nanoparticles

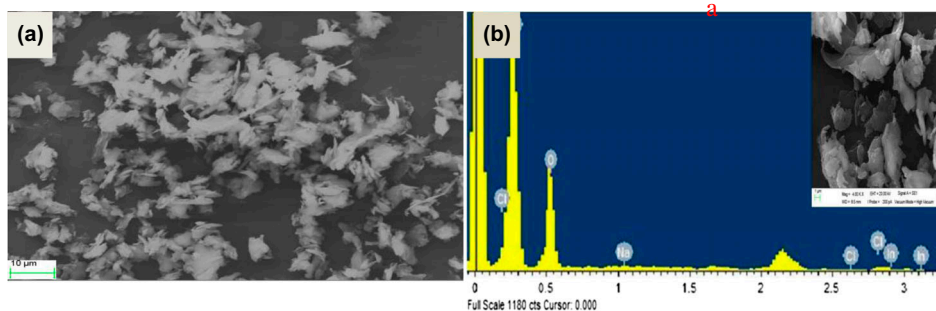


Figure 1. (a) Scanning electron microscopy and (b) energy-dispersive X-ray spectroscopy analysis of oil palm shell nanoparticles.

using high-energy ball milling process. Guo and Lua [32] observed that the OPS nanoparticles have a similar porosity with sufficient solid density in both angular and irregular structural shaped. Similarly, Dungani et al. [33] reported the crushed and irregular structural shape of the OPS nanoparticles due to ball milling process. The elemental composition of the OPS nanoparticles was determined by SEM equipped with energy dispersive X-ray analysis (SEM–EDX), as presented in Figure 1(b). Result shows that the presence of carbon (67.47 wt.%) and oxygen (43.04 wt.%) in the OPS nanoparticle as major elements. Other elemental compositions detected in the OPS nanoparticle are sodium, chlorine, and indium. Similarly, Dagwa et al. [34] reported the presence of carbon (63.02%) and oxygen (36.04%) as major elements in the OPS nanoparticle.

Figure 2(a) presents the TEM image of OPS nanoparticles. The micrograph reveals nanometric irregular shape formation of the OPS nanoparticles with size between 10 and 30 nm, without having any agglomeration. Moreover, the particle size analysis revealed the wide range of particle size distribution of OPS nanoparticles (Figure 2(b)). The average diameter of OPS nanoparticles was within the range of 50.75–91.28 nm. It was found that the size distribution intensity of OPS nanoparticles was 75.30%. XRD analysis of OPS was conducted to investigate the CI of the fillers. The XRD pattern of OPS nanoparticles is shown in Figure 3(a). However, the crystalline index of OPS nanoparticles was found to be 34.56 %. This result proved that the OPS nanoparticles had a crystalline nature with a lower degree of crystalline index.

The thermal decomposition curves of OPS nanoparticles, analyzed by TGA, are shown in Figure 3(b). It was observed that first stage of degradation occurred at temperature below 100 °C, probably due to the evaporation of moisture present in the sample. Meanwhile, the second stage of degradation occurred at temperature of 200–500 °C. The weight loss at this temperature region corresponds to the formation of volatile product that arose from random scission and intermolecular transfer involving tertiary hydrogen abstractions from hemicelluloses, cellulose, and lignin.[35] In this study,  $T_{10\%}$  and  $T_{50\%}$  were determined in the thermal degradation process OPS nanoparticles at 10% and 50% weight losses, respectively. Wherein,  $T_{10\%}$  is selected as

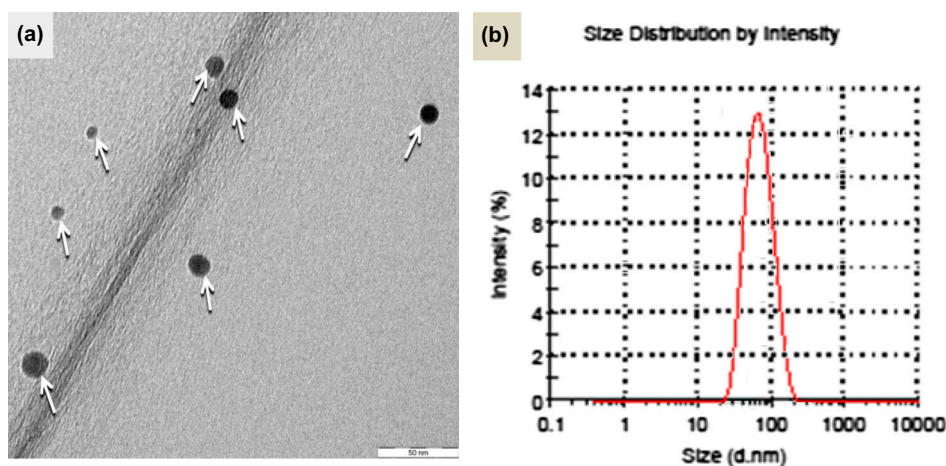


Figure 2. Particle size analysis of OPS nanoparticles (a) TEM images of OPS nanoparticle; (b) particle size distributions of OPS nanoparticles.

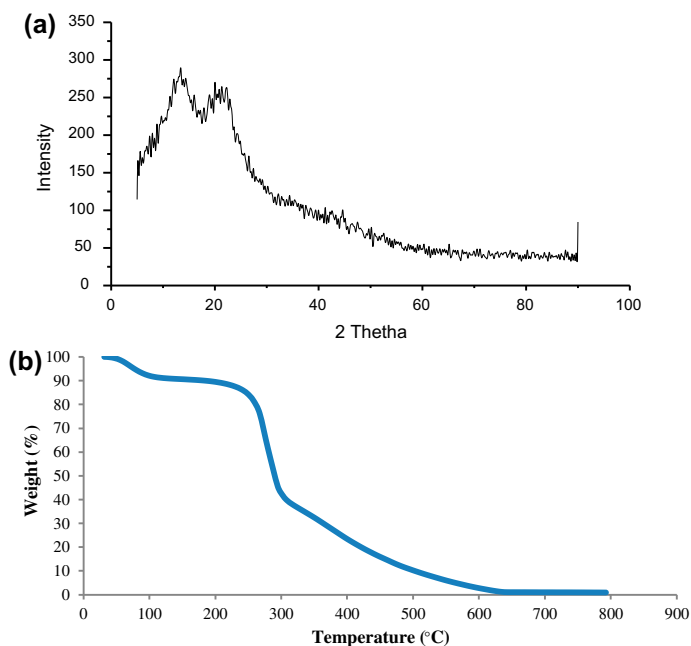


Figure 3. X-ray diffraction pattern (a) and thermogravimetric curve (b) of oil palm shell nanoparticles.

$T_{\text{onset}}$ . It was observed that  $T_{10\%}$  and  $T_{50\%}$  weight loss occurred at temperature of 187 °C and 280 °C, respectively. The constant weight was found at a temperature of 600–800 °C. However, the total residual content was determined to be 0.84% at 800 °C.

### 3.2. OPS nanofiller in fiber-reinforced polyester hybrid composites

#### 3.2.1. Physical properties

The physical properties of the hybrid composites including density, void content, and water absorption were analyzed by varying the filler loading. Table 1 presents influence of OPS nanoparticles on density (theoretical and experimental) and void content of natural fiber reinforcement hybrid composites. It was observed that the density increased with filler loading. The density for hybrid composites without filler was 1.125 g/cm<sup>3</sup>.

Table 1. Influence of OPS nanoparticles on density and voids content of natural fiber-reinforced hybrid composites.

Filler loading (wt.%)	Theoretical density (g/cm <sup>3</sup> )	Measured density (g/cm <sup>3</sup> )	Void content (%)
Control	1.186 ± 0.053*	1.125 ± 0.046	5.143 ± 0.035
1	1.189 ± 0.021	1.133 ± 0.024	4.710 ± 0.048
3	1.196 ± 0.043	1.137 ± 0.016	4.933 ± 0.052
5	1.209 ± 0.035	1.141 ± 0.024	5.624 ± 0.062

\* Standard deviation.

Meanwhile, density of hybrid composites by adding OPS nanoparticles from 1 to 5% increased the density from 1.133 to 1.141 g cm<sup>-3</sup>. This finding indicated the hybridization of OPS nanoparticles into fibers reinforced hybrid composites would increase the density. However, the measured density values of hybrid composites slightly varied with the theoretical density values, which might be due to the presence of voids in composites.[3]

The void content of the composites decreased with increasing filler up to 3% from 5.143 to 4.933% (Table 1). This because of the OPS nanoparticles might filled into the void in matrix, which may reduce the void content of composites.[26] Homogenous dispersion of filler in polyester resin is also a possible reason for this low void content of hybrid-prepared composites. On the contrary, the hybrid composites with the incorporation of 5% filler loading had the highest void content (5.624%). This was probably due to the particle-to-particle interaction rather than particle-to-polymer interaction with higher amount of OPS nanoparticles at 5% loading. The particles tend to agglomerate and create lumps which affected the interaction between polymer chains and reduced the cross linking, thereby increasing the void content in polymer itself.[8]

### 3.2.2. Mechanical properties

The influence of OPS nanoparticles on the mechanical properties including tensile properties, flexural properties, and impact properties of hybrid composites was evaluated, as presented in Tables 2 and 3. It was observed that the tensile properties such as tensile strength, tensile modulus, and tensile toughness increased with increasing nanoparticles loading up to 3% and decreased thereafter (Table 2). Hybrid composites without the addition of nanoparticles contributed the lowest tensile strength (30.10 MPa), tensile modulus (0.77 GPa), and tensile toughness (38.76 J/m<sup>3</sup>). However, the addition of OPS nanofiller into the composite increased the tensile strength, tensile modulus, and tensile toughness of hybrid composite. Wherein, the highest tensile strength (37.56 MPa), tensile modulus (1.15 GPa), and tensile toughness (46.21 J/m<sup>3</sup>) were gained at 3% OPS nanoparticles loading into the hybrid composite. This result indicated the addition of nanoparticles in composites played a role in increasing surface area, energy absorbing capability, and minimizing free space within the hybrid composite, thereby enhanced tensile properties. This indicates that 3% filler loading of the OPS nanoparticles successfully increased the optimum polyester ability to transmit and to distribute stress. Moreover, this scenario was also probably due to uniform dispersion of OPS nanoparticles in matrix, which creates better filler–matrix interaction and interface region with fibers. Thus, the loading transfer became easier and the sample was able to sustain

Table 2. Influence of tensile properties with OPS nanofiller loading on natural fiber-reinforced hybrid composite.

	Control	OPS nanoparticles		
		1 wt.%	3 wt.%	5 wt.%
Tensile strength (MPa)	30.10 ± 1.03	33.07 ± 1.26	37.56 ± 1.12	34.02 ± 1.08
Tensile modulus (GPa)	0.76 ± 0.04	0.91 ± 0.06	1.15 ± 0.05	1.03 ± 0.06
Tensile toughness (J/m <sup>3</sup> )	38.76 ± 1.24	41.82 ± 1.54	46.21 ± 1.25	39.15 ± 1.16
Elongation at break (%)	6.06 ± 0.36	5.58 ± 0.28	5.18 ± 0.42	4.25 ± 0.46

± Standard deviation.

Table 3. Influence of flexural properties with OPS nanofiller loading on natural fiber-reinforced hybrid composite.

Flexural properties and impact test	Control	OPS nanoparticles		
		1 wt.%	3 wt.%	5 wt.%
Flexural strength (MPa)	60.42 ± 2.19	65.3 ± 2.14	75.27 ± 2.43	69.45 ± 2.12
Flexural modulus (GPa)	4.41 ± 0.24	4.88 ± 0.46	6.17 ± 0.38	5.39 ± 0.18
Flexural toughness (J/m <sup>3</sup> )	45.76 ± 1.58	49.82 ± 1.62	56.21 ± 1.06	46.15 ± 1.38
Izod notched impact test (kJ/m <sup>2</sup> )	10.84 ± 0.56	12.01 ± 0.68	13.42 ± 0.49	12.72 ± 0.64

± Standard deviation.

more load resulting in higher tensile strength of hybrid composites. Homogenous dispersion of particles gave better filler–matrix interaction and better interface adhesion with fibers as well resulting increases in energy absorption. The decrease in tensile properties (tensile strength, tensile modulus, and tensile toughness) with an increase in OPS nanofiller from 3 to 5% was due to the agglomeration of the nanofiller with higher loading, which influences the stress transfer mechanism and poor wetting of the polymer systems.[36] The poor wetting between fibers and filler/matrix influenced tendency of voids formation in composites, which can be a stress point to reduce the tensile properties of composites. According to Neitzel et al.,[37] nanoparticles have a strong tendency to gather each other and formed some aggregation, thus minimized their surface area. The agglomerated filler particles would decrease filler–matrix interaction as a result of reduced fiber–matrix adhesion interface.

The percentage elongation at break decreased with an increase in OPS nanoparticles loading (Table 2). The high elongation at break (6.06%) was obtained without filler loading in hybrid composites. Meanwhile, 5% filler loading had gained the lowest elongation at break (4.25%). This phenomenon might have occurred due to the high rigidity of the OPS nanostructure rather than the matrix. As high rigidity of OPS filler loading increased, it would restrict the chain mobility of matrix that was available for elongation.[36] Thus, it lead to higher breaking tendency (lower deformation) of the composites which in turn decreased the percentage elongation at break of composite. The increase in filler loading resulted in reduction of elongation at break which might be due to the decrease in deformability of interface between filler and the matrix.[37]

Table 3 represents the flexural properties including strength, modulus, and toughness hybrid composites with the incorporation of OPS nanoparticles. The flexural properties exhibit a similar behavior with tensile properties. It was observed that the flexural properties increased with increasing the OPS nanoparticles loading up to 3%. However, an increase in OPS nanoparticles loading from 3 to 5%, decreased the flexural properties of the hybrid composite. The rate of the inter-particle interactions of the nanoparticles in composites is crucial, which may attribute to this trend of results.[23] It is understandable that homogeneous dispersion of filler improves interfacial interaction between filler and matrix hence reduces flexibility of chain polymer. Furthermore, the increasing filler loading means higher surface area of the filler which increases effective bonding between fillers/matrix and results in higher flexural modulus of the composites.[36] Factor level of dispersion of nanoparticles in matrix influenced increment by flexural toughness properties. Therefore, the decrease in flexural properties with an increase in OPS nanofiller from 3 to 5% might be due to the agglomeration of

the nanofiller, which influences the stress transfer mechanism and high viscosity of polymer systems.[36, 26]

The impact strength of hybrid composites was found to increase with the increase in filler loading (Table 3). The high impact strength ( $13.5 \text{ kJ/m}^2$ ) of the hybrid composites was observed at 3% filler loading. Higher impact strength of nanocomposites is related with the rate dispersion of the nanofiller. Excellent homogeneous dispersion of nanofiller increased filler–matrix interaction and creates good interfacial adhesion with fibers. Hence, energy would be absorbed easily and crack propagation would be prevented, thus improving impact strength. In contrast, poor nanofiller dispersion increases the tendency of particles to agglomerate thus minimizing their surface area. The agglomerated particles disturb the formation of better adhesion region between fiber and matrix, and therefore reduce the efficiency of energy absorption during crack propagation. This phenomenon explained the decrease in impact strength at 5% OPS nanoparticles loading into hybrid composite.

### 3.2.3. Morphology properties

Figure 4 shows SEM images of the tensile fracture surface of natural fiber-reinforced polyester composite with the incorporation of OPS nanoparticles. It was observed that the nanoparticles were not exhibited in the SEM micrographs of composites. This might be due to the effective amalgamation of OPS nanoparticles with the matrix. It was apparent that the fiber detachment and voids formation without loading filler in hybrid composites implied weak adhesion between the fiber and the matrix (Figure 4(a)). The addition of OPS nanoparticles into the composite influenced the composite properties in Figure 4(b–d). At 1% OPS nanofiller loading (Figure 4(b)), it was observed that the surface of the hybrid composites became smooth with minimizing the fiber detachment. Although, skin matrix formation of the composite was observed, the adhesion between fiber and matrix was poor. The presence of clean fiber pulling out from the composite was detected and there is a small gap between fibers and matrix (Figure 4(b)). Better skin matrix formation of the composite was observed with the increase in the OPS nanofiller loading from 1 to 3% (Figure 4(c)). Further, absence of fiber pulling out from the composite and the gap between fibers and matrix indicates effective adhesion between fiber and matrix in the hybrid composites. However, there were some voids and fiber fracture was observed at 3% nanoparticles loading into the composite. Further increase in OPS nanoparticles loading from 3 to 5%, occurrence of the fiber detachment and higher number of voids were detected in the hybrid composites (Figure 4(d)). The increase in the fiber pull out voids and the fiber detachment on the surface of natural fiber-reinforced polyester composite were probably due to the poor wetting of the fiber do higher OPS nanoparticles content in the polymer matrix.[38]

### 3.2.4. Thermal properties

Figure 5 shows the influence of OPS nanoparticles into natural fiber-reinforced polyester hybrid composites. It was observed that the composites had two-stage degradations. Wherein, first-stage degradation occurred below the temperature of  $100 \text{ }^\circ\text{C}$  and second-stage degradation was observed at a temperature range of  $200\text{--}550 \text{ }^\circ\text{C}$ . The thermal degradation temperatures ( $T_{10\%}$  and  $T_{50\%}$ ) and percentage of the char residue of hybrid composites are tabulated in Table 4. It was observed that the thermal stability of hybrid

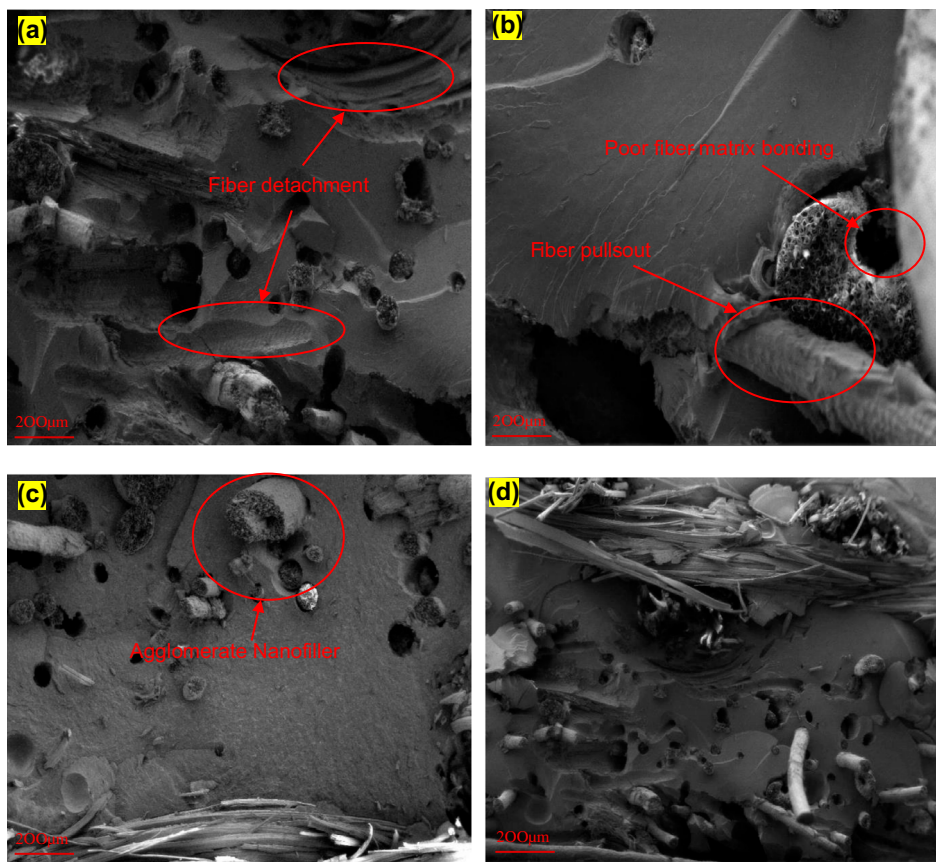


Figure 4. Scanning electron microscopy images of natural fiber-reinforced hybrid composite with the incorporation of OPS nanoparticles. (a) Control; (b) 1 wt.% OPS nanoparticles; (c) 3 wt.% OPS nanoparticles; (d) 5 wt.% OPS nanoparticles.

composites increased with increasing OPS nanoparticles loading into the thermal stability up to 3% and decreased with further increase in the nanoparticles loading (Figure 5 and Table 4). Results indicated that the incorporation of OPS nanoparticles enhanced the thermal stability of the natural fiber-reinforced polyester hybrid composites. This was because of the inter-particle interaction of OPS nanoparticles consumed heat from the matrix, hence improved the thermal stability of hybrid composites.[39] However, the reduction of the thermal degradation temperature at 5% OPS nanofiller loading into the natural fiber-reinforced polyester hybrid composites might be due to the agglomeration of OPS nanoparticles, which leads to a decrease in the molecular mobility restriction.[40] The decomposition of cellulosic materials at higher temperatures generates a carbonaceous residue, which is known as char, which forms as a barrier heat source and polymeric materials. It was found that the percentage char residue increased with increasing OPS nanoparticles into hybrid composite (Table 4). However, the highest percentage of char residue was detected at 3% OPS nanoparticles loading into the hybrid composite. The char residue may correspond to the lignin and cellulose content in the hybrid composite.

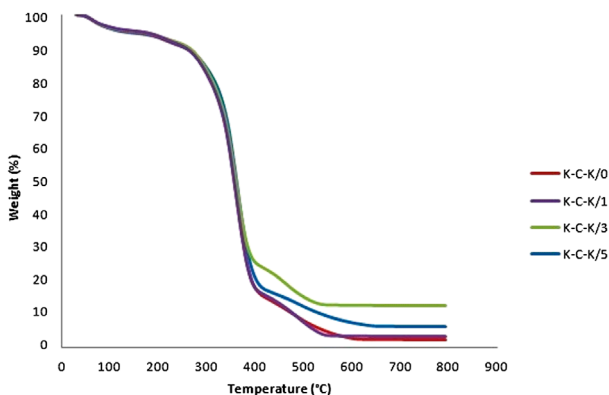


Figure 5. TGA curve on the effect of oil palm shell nanofiller loading in natural fiber-reinforced hybrid polyester composites.

Table 4. Influence of the OPS nanofiller on thermal degradation temperature of natural fiber-reinforced polyester hybrid composites.

Nanofiller loading (wt.%)	Degradation temperature (°C)		Char residue (%)
	$T_{10\%}$	$T_{50\%}$	
Control	240	346	0.8
1	247	353	1.0
3	265	355	11.0
5	256	354	6.5

#### 4. Conclusions

The OPS nanoparticles were successfully prepared from the OPS by ball milling process. The analysis of the fundamental properties of the prepared OPS nanoparticles revealed that the OPS nanoparticles contain a high amount of carbon and oxygen. The crystalline index of the OPS nanoparticles was found to be 34.56%. In the present study, OPS nanoparticles were utilized as natural filler in order to enhance the physical, mechanical, and thermal properties of the natural fibers reinforced polyester hybrid composites. Results showed that the OPS nanoparticles had the potential to be used as natural filler in place of synthetic fillers. Further, 3 wt.% OPS nanoparticles loading into the natural fibers reinforced polyester hybrid composites had the optimal physical, mechanical, and thermal characteristics of the hybrid composite. The analysis of fracture surface using SEM revealed the presence of fiber pulling out, voids and fiber fracture at 3 wt.% OPS nanoparticles loading into the composite. However, this minimal incompatibility between nanoparticles and matrix at 3 wt.% OPS nanoparticles loading into the hybrid composites could be overcome by treating the fiber with coupling agent.

#### Acknowledgment

The authors would like to thank the Universiti Sains Malaysia for providing Research University Grant (RUI) (No.: 1001/PTEKIND/814255) as a financial support.

### Disclosure statement

No potential conflict of interest was reported by the authors.

### Funding

This work was supported by Universiti Sains Malaysia [grant number 1001/PTEKIND/814255].

### References

- [1] Alwani MS, Khalil HPS, Islam MN, et al. Microstructural study, tensile properties, and scanning electron microscopy fractography failure analysis of various agricultural residue fibers. *J. Nat. Fibers*. 2015;12:154–168.
- [2] George J, Sreekala MS, Thomas S. A review on interface modification and characterization of natural fiber reinforced plastic composites. *Polym. Eng. Sci.* 2001;41:1471–1485.
- [3] Jawaid M, Abdul Khalil HPS. Cellulosic/synthetic fibre reinforced polymer hybrid composites: a review. *Carbohydr. Polym.* 2011; 86: 1–18.
- [4] Joshi SV, Drzal LT, Mohanty AK, et al. Are natural fiber composites environmentally superior to glass fiber reinforced composites? *Composites Part A*. 2004;35:371–376.
- [5] O'Donnell A, Dweib MA, Wool RP. Natural fiber composites with plant oil-based resin. *Compos. Sci. Technol.* 2004;64:1135–1145.
- [6] Fatah IYA, Khalil HPS, Hossain MS, et al. Exploration of a chemo-mechanical technique for the isolation of nanofibrillated cellulosic fiber from oil palm empty fruit bunch as a reinforcing agent in composites materials. *Polymers*. 2014;6:2611–2624.
- [7] Khalil HPS, Tehrani MA, Davoudpour Y, et al. Natural fiber reinforced poly(vinyl chloride) composites: a review. *J. Reinf. Plast. Compos.* 2013;32:330–356.
- [8] Cheung H-Y, Ho MP, Lau K-T, et al. Natural fibre-reinforced composites for bioengineering and environmental engineering applications. *Composites Part B*. 2009;40:655–663.
- [9] Farag MM. Quantitative methods of materials substitution: application to automotive components. *Mater. Des.* 2008;29:374–380.
- [10] Jawaid M, Othman A, Saba N, et al. Effect of chemical modifications of fibers on tensile properties of epoxy hybrid composites. *Int. J. Polym. Anal. Charact.* 2014; 19:391–403
- [11] John MJ, Thomas S. Biofibres and biocomposites. *Carbohydr. Polym.* 2008;71:343–364.
- [12] Panthapulakkal S, Zereskian A, Sain M. Preparation and characterization of wheat straw fibers for reinforcing application in injection molded thermoplastic composites. *Bioresour. Technol.* 2006;97:265–272.
- [13] Pradhan S, Costa FR, Wagenknecht U, et al. Elastomer/LDH nanocomposites: synthesis and studies on nanoparticle dispersion, mechanical properties and interfacial adhesion. *Eur. Polym. J.* 2008;44:3122–3132.
- [14] Tjong SC. Structure, morphology, mechanical and thermal characteristics of the *in situ* composites based on liquid crystalline polymers and thermoplastics. *Mater. Sci. Eng., R*. 2003;41:1–60.
- [15] Dittenber DB, GangaRao HVS. Critical review of recent publications on use of natural composites in infrastructure. *Composites Part A*. 2012;43:1419–1429.
- [16] Yasmin A, Daniel IM. Mechanical and thermal properties of graphite platelet/epoxy composites. *Polymer*. 2004;45:8211–8219.
- [17] Debelak B, Lafdi K. Use of exfoliated graphite filler to enhance polymer physical properties. *Carbon*. 2007;45:1727–1734.
- [18] Fiedler B, Gojny FH, Wichmann MHG, et al. Fundamental aspects of nano-reinforced composites. *Compos. Sci. Technol.* 2006;66:3115–3125.
- [19] Dastjerdi R, Montazer M. A review on the application of inorganic nano-structured materials in the modification of textiles: focus on anti-microbial properties. *Colloids Surf., B*. 2010;79:5–18.
- [20] Araj MT, Shakour SA. Realizing the environmental impact of soft materials: criteria for utilization and design specification. *Mater. Des.* 2013;43:560–571.
- [21] Dowling AP. Development of nanotechnologies. *Mater. Today*. 2004;7:30–35.

- [22] Akil HM, Omar MF, Mazuki AAM, et al. Kenaf fiber reinforced composites: a review. *Mater. Des.* 2011;32:4107–4121.
- [23] Chapple S, Anandjiwala R. Flammability of natural fiber-reinforced composites and strategies for fire retardancy: a review. *J. Thermoplast. Compos. Mater.* 2010;23:871–893.
- [24] La Mantia FP, Morreale M. Green composites: a brief review. *Composites Part A.* 2011;42:579–588.
- [25] Gutiérrez LF, Sánchez ÓJ, Cardona CA. Process integration possibilities for biodiesel production from palm oil using ethanol obtained from lignocellulosic residues of oil palm industry. *Bioresour. Technol.* 2009;100:1227–1237.
- [26] Njuguna J, Pielichowski K, Desai S. Nanofiller-reinforced polymer nanocomposites. *Polym. Adv. Technol.* 2008;19:947–959.
- [27] ASTM D. Standard test methods for apparent density, bulk factor, and pourability of plastic materials. West Conshohocken (PA): ASTM International; 1996.
- [28] ASTM D. Standard test method for void content of reinforced plastics. West Conshohocken (PA): ASTM International; 1999.
- [29] ASTM D. Standard test method for tensile properties of polymer matrix composite materials. West Conshohocken (PA): ASTM International; 2000.
- [30] ASTM D. Standard test methods for flexural properties of unreinforced and reinforced plastics and electrical insulating materials. West Conshohocken (PA): ASTM International; 2003.
- [31] ASTM D. Standard test method for determining the izod pendulum impact resistance of plastics. West Conshohocken (PA): ASTM International; 2006.
- [32] Guo J, Lua AC. Characterization of adsorbent prepared from oil-palm shell by CO<sub>2</sub> activation for removal of gaseous pollutants. *Mater. Lett.* 2002;55:334–339.
- [33] Dungani R, Islam MN, Abdul Khalil HPS, et al. Modification of the inner part of the oil palm trunk (OPT) with oil palm shell (OPS) nanoparticles and phenol formaldehyde (PF) resin: physical, mechanical, and thermal properties. *Bioresources.* 2014; 9:455–471.
- [34] Dagwa I, Builders P, Achebo J. Characterization of palm kernel shell powder for use in polymer matrix composites. *Int J Mech Mechatronics Eng.* 2012;12:88–93.
- [35] Ghasemi I, Kord B. Long-term water absorption behaviour of polypropylene/wood flour/organoclay hybrid nanocomposite. *Iran Polym. J.* 2009;18:683–691.
- [36] Faruk O, Bledzki AK, Fink H-P, et al. Progress report on natural fiber reinforced composites. *Macromol. Mater. Eng.* 2014;299:9–26.
- [37] Neitzel I, Mochalin V, Knoke I, et al. Mechanical properties of epoxy composites with high contents of nanodiamond. *Compos. Sci. Technol.* 2011;71:710–716.
- [38] Dasari A, Yu Z-Z, Mai Y-W. Fundamental aspects and recent progress on wear/scratch damage in polymer nanocomposites. *Mater. Sci. Eng., R.* 2009;63:31–80.
- [39] He H, Li K, Wang J, et al. Study on thermal and mechanical properties of nano-calcium carbonate/epoxy composites. *Mater. Des.* 2011;32:4521–4527.
- [40] Zhou T, Wang X, Gu M, Xiong D. Study on mechanical, thermal and electrical characterizations of Nano-SiC/Epoxy composites. *Polym J.* 2008;41:51–57.